

Supporting Information

for

Piezochromic Luminescent Behaviors of Two New Benzothiazole-enamido Boron Difluoride Complexes: Intra- and Inter-molecular Effects Induced by Hydrostatic Compression

Xiaoqing Wang,^a Qingsong Liu,^a Hui Yan,^a Zhipeng Liu,^{a,*} Mingguang Yao,^{b,*} Qingfu Zhang,^a Shuwen Gong,^a and Weijiang He^{c,*}

^a*Institute of Functional Organic Molecules and Materials, School of Chemistry and Chemical Engineering, School of Material Science and Engineering, School of Pharmacy, Liaocheng University, Hunan Road No.1, Liaocheng, 252000, P.R. China; E-mail: chliuzp@163.com.*

^b*National Laboratory of Superhard Materials, Institute of Atomic and Molecular Physics, Jilin University, Changchun 130012, People's Republic of China; E-mail: yaomg@jlu.edu.cn.*

^c*State Key Laboratory of Coordination Chemistry, Coordination Chemistry Institute, School of Chemistry and Chemical Engineering, Nanjing University, Hankou Road No.22, Nanjing, 210093, P.R. China. E-mail: heweij69@nju.edu.cn.*

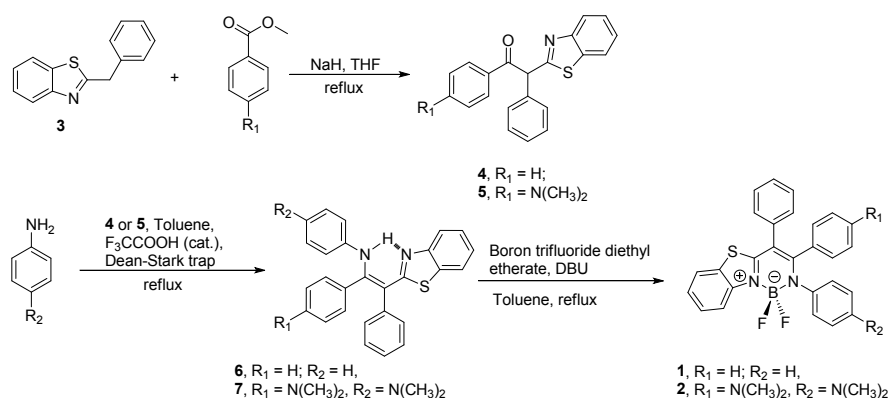
Contents:

- 1. General methods and materials.**
- 2. Synthesis of compounds 1 and 2.**
- 3. Absorption and luminescence spectroscopic studies of compounds 1 and 2**
- 4. Luminescent response of compounds 1 and 2 to the mechanical grinding**
- 5. Luminescence of compounds 1 and 2 upon hydrostatic compression**
- 6. X-ray crystallographic analysis**
- 7. Single-point DFT calculations of Compounds 1 and 2.**
- 8. Molecular packing modes optimized by DFT**
- 9. References**
- 10. NMR Spectra**

1. General methods and materials.

All the air-sensitive compound-involved reactions and manipulations were carried out in an atmosphere of dry argon by using Schlenk techniques and/or vacuum line techniques. Solvents were dried prior to use by the common methods in organometallic chemistry. Chemicals were commercially obtained and used as received. ^1H , ^{11}B and ^{13}C NMR spectra were recorded using Varian Mercury-plus 400M spectrometer. Chemical shifts were reported in ppm relative to $\text{Si}(\text{CH}_3)_4$ (^1H , ^{13}C) or $\text{BF}_3\cdot\text{Et}_2\text{O}$ (^{11}B), respectively, and coupling constants (J) were given in Hz. Mass spectra were obtained on a LCQ (ESI-MS, Thermo Finnigan) mass spectrometer. Column chromatography was performed using silica gel (200 mesh, Qingdao Haiyang Chemical Co., Ltd).

2. Synthesis of compounds 1 and 2.



Scheme S1. Synthetic scheme of compounds 1 and 2.

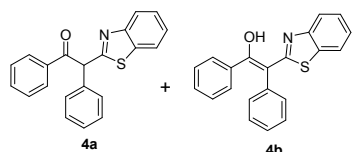
Synthesis of 2-Benzylbenzothiazole (3)

A mixture of 2-aminothiophenol (10.8 mL, 100 mmol) and phenylacetic acid (20.4 g, 150 mmol) were heated to 240 °C for 2 h. After cooling to room temperature, the resulted mixture was purified with column chromatography on silica gel (Ethyl acetate: Petroleum ether = 1: 10, $R_f = 0.4$) to give **3** (79%, 17.8 g) as yellow oil. ^1H NMR (400 MHz, CDCl_3): δ /ppm = 8.00 (d, $J = 8.2$ Hz, 1H), 7.79 (d, $J = 7.9$ Hz, 1H), 7.46 (t, $J = 7.7$ Hz, 1H), 7.41–7.28 (m, 6H), 4.45 (s, 2H).

General procedure for the synthesis of compounds 4 and 5.

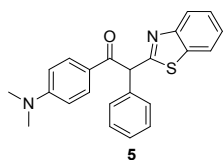
Compound **3** was added to a mixture of THF and NaH (60w% in oil, 100 mmol) at room temperature. After being stirred for 20 minutes, the mixture was added with methyl benzoate or methyl 4-(dimethylamino)benzoate, and the mixture was refluxed for 10 h. Then the mixture was cooled to room temperature, and 2 M HCl was added slowly, and the yellow precipitate was formed. The product was obtained as yellow solid via filtration, washing and drying.

Compound 4

	Batch		
	3	1.92 g	8.5 mmol
	methyl benzoate	1.23 g	11.0 mmol
	NaH	1.0 g	25.0 mmol
	THF	15 mL	

A mixture of **4a** and **4b** was obtained (**4a**: **4b** = 1: 2); Yield: 90% (2.5 g), ¹H NMR (400 MHz, CDCl₃): δ/ppm = 8.07 (d, *J* = 7.9 Hz, 2H), 8.00 (d, *J* = 8.1 Hz, 1H), 7.88–7.83 (m, 6H), 7.70 (d, *J* = 7.9 Hz, 3H), 7.54 (d, *J* = 7.1 Hz, 3H), 7.45 (dd, *J* = 12.9, 7.1 Hz, 7H), 7.41–7.09 (m, 42H), 6.60 (s, 1H).

Compound 5



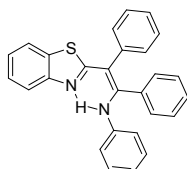
Batch		
3	3.5 g	15.5 mmol
methyl 4-(dimethylamino)benzoate	2.92 g	16.3 mmol
NaH	1.9 g	47.5 mmol
THF	20 mL	

Yield: 92% (5.3 g), ¹H NMR (400 MHz, CDCl₃) δ/ppm = 8.03 (d, *J* = 8.2 Hz, 1H), 7.62 (d, *J* = 7.9 Hz, 1H), 7.42 (t, *J* = 7.8 Hz, 1H), 7.31–7.17 (m, 5H), 7.12 (d, *J* = 8.9 Hz, 3H), 6.46 (d, *J* = 8.8 Hz, 2H), 5.87 (s, 1H), 2.92 (s, 6H). ¹³C NMR (100 MHz, CDCl₃): δ/ppm = 163.8, 161.7, 150.8, 143.6, 143.1, 130.6, 128.7, 128.4, 128.2, 127.7, 127.4, 125.7, 124.4, 123.3, 121.5, 117.7, 111.1, 40.1.

General procedure for the synthesis of compounds 6–7.

Ketone (**4** or **5**, 1 equiv.), aniline (2 equiv.) and toluene were added to a round bottom flask equipped with a Dean-Stark trap and condenser. Then 2 drops of trifluoroacetic acid (cat. amount) was added with stirring. The resulted solution was reflux for 12 h. After being cooled to room temperature, toluene was removed *in vacuo*. The residue was purified with column chromatography on silica gel to give desired product as yellow solid.

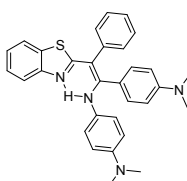
Compound 6



Batch		
4	685 mg	2.08 mmol
Aniline	387 mg	4.15 mmol
toluene	15 mL	

Yield: 67% (565 mg), ¹H NMR (400 MHz, CDCl₃) δ/ppm = 12.51 (s, 1H), 8.05–7.81 (m, 1H), 7.69 (dd, *J* = 7.9, 0.4 Hz, 1H), 7.5–7.28 (m, 1H), 7.30–7.15 (m, 5H), 7.18–6.96 (m, 6H), 6.90 (t, *J* = 7.4 Hz, 1H), 6.74 (d, *J* = 7.9 Hz, 2H); ¹³C NMR (100 MHz, CDCl₃): δ/ppm = 171.9, 153.7, 148.9, 141.34, 139.6, 135.3, 133.0, 130.52, 128.7, 128.2, 128.0, 127.8, 127.1, 125.9, 123.6, 122.4, 122.1, 121.0, 120.9, 107.4.

Compound 7



Batch		
5	1.42 g	3.81 mmol
Aniline	1.04 g	7.61 mmol
Toluene	15 mL	

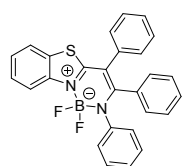
Yield: 36% (678 mg), ¹H NMR (400 MHz, CDCl₃) δ/ppm = ¹H NMR (400 MHz, CDCl₃) δ 12.34 (s, 1H), 7.80 (d, *J* = 8.1 Hz, 1H), 7.62 (d, *J* = 7.9 Hz, 1H), 7.35 (t, *J* = 7.8 Hz, 1H), 7.28–7.10 (m, 6H), 6.91 (d, *J* = 8.7 Hz, 2H), 6.72 (d, *J* = 8.8 Hz, 2H), 6.55 (d, *J* = 8.9 Hz, 2H), 6.35 (d, *J* = 8.7 Hz, 2H), 2.85 (s, 6H), 2.84 (s, 6H); ¹³C NMR (100 MHz, CDCl₃):

δ /ppm = 172.2, 153.9, 151.1, 149.6, 146.6, 140.8, 133.1, 132.9, 131.9, 131.7, 131.6, 128.1, 126.6, 125.7, 125.6, 123.9, 123.8, 122.9, 122.8, 120.7, 120.6, 120.5, 120.4, 113.4, 113.2, 111.2, 111.1, 105.3, 41.2, 40.2.

General procedure for the synthesis of compounds 1 and 2.

After dissolving enamide (**6** or **7**, 1 equiv.) in dry toluene, DBU (3 equiv.) was added to the solution and stirred for 10 minutes at room temperature. A solution of toluene containing of boron trifluoride diethyl ether complex (5 equiv.) was slowly added to the mixture via syringe. Then the mixture was refluxed for 1 h followed by cooling to room temperature. The mixture was extracted with dichloride methane, and the collected dichloride methane layer was washed with water and brine. After being dried over anhydrous magnesium sulfate, the solution was filtrated though a short pad of silica gel. Removing the solvent yielded the product with high purity.

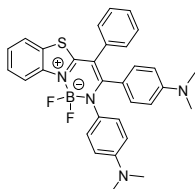
Compound 1



Batch		
6	314 mg	0.78 mmol
BF ₃ ·O(Et) ₂	550 mg	3.88 mmol
DBU	354 mg	2.33 mmol
Toluene	15 mL	

Yield: 85% (300 mg), ¹H NMR (400 MHz, CDCl₃) δ /ppm = 8.12 (d, *J* = 8.4, 1H), 7.58 (d, *J* = 8.1, 1H), 7.51–7.44 (m, 1H), 7.30 (dd, *J* = 10.9, 4.4, 1H), 7.24–7.12 (m, 9H), 7.07 (dd, *J* = 11.2, 4.1, 1H), 6.97–6.87 (m, 5H); ¹³C NMR (100 MHz, CDCl₃): δ /ppm = 162.5, 155.4, 139.4, 137.3, 132.5, 130.2, 127.2, 125.4, 124.3, 124.0, 123.5, 123.3, 122.9, 122.9, 122.6, 121.6, 120.1, 116.7, 113.5, 98.8; ¹¹B NMR (128 MHz, CDCl₃): δ /ppm = 2.19 (t, *J* = 30.3 Hz). ESI-MS: calcd., [M+Na]⁺ = 475.32, found: [M+Na]⁺ = 475.67.

Compound 2



Batch		
7	408 mg	0.83 mmol
BF ₃ ·O(Et) ₂	590 mg	4.16 mmol
DBU	378 mg	2.49 mmol
Toluene	15 mL	

Yield: 90% (402 mg), ¹H NMR (400 MHz, CDCl₃) δ /ppm = 8.05 (d, *J* = 8.2 Hz, 1H), 7.50 (d, *J* = 7.9 Hz, 1H), 7.41 (t, *J* = 7.8 Hz, 1H), 7.25–7.19 (m, 3H), 7.15 (m, 3H), 7.03 (d, *J* = 8.7 Hz, 2H), 6.74 (d, *J* = 8.7 Hz, 2H), 6.55 (d, *J* = 8.8 Hz, 2H), 6.22 (d, *J* = 8.7 Hz, 2H), 2.86 (s, 6H), 2.79 (s, 6H); ¹³C NMR (100 MHz, CDCl₃): δ /ppm = 166.2, 161.3, 149.5, 148.5, 144.3, 138.4, 132.2, 131.8, 131.6, 131.5, 128.9, 128.6, 127.9, 127.2, 127.0, 124.1, 122.5, 121.1, 117.8, 112.5, 112.4, 110.6, 110.5, 103.2, 40.9, 40.8, 40.1, 40.0; ¹¹B NMR (128 MHz, CDCl₃): δ /ppm = 2.17 (t, *J* = 30.2 Hz). ESI-MS: calcd., [M+Na]⁺ = 561.46, found: [M+Na]⁺ = 561.75.

3. Absorption and luminescence spectroscopic studies of compounds 1 and 2

Spectra of solutions

UV-vis absorption spectra were recorded on a Shimadzu UV-3600 spectrometer with a resolution of 1.0 nm. A solution of the sample (*ca.* 10⁻⁵ M) in a 1 cm quartz cuvette was used for the measurement. Fluorescence spectra were recorded on a Hitachi F-7000 spectrometer under following conditions. λ_{ex} , 395 nm (**1**); 409 nm (**2**); both the

excitation and emission slits are 8 nm, and the PMT voltage is 650 V.

Spectra of solids

Powder samples of **1** and **2** were used for the determination. The fluorescence lifetimes and the absolute quantum yields (Φ_f) of the powder samples were determined with a Horiba Jobin Yvon Fluorolog-3 spectrofluorimeter. Fluorescence quantum yield of compounds **1** and **2** in solution were determined by using 4-methylamino-7-nitro-2,1,3-benzoxadiazole ($\Phi_f = 0.38$ in acetonitrile) as reference.^[1]

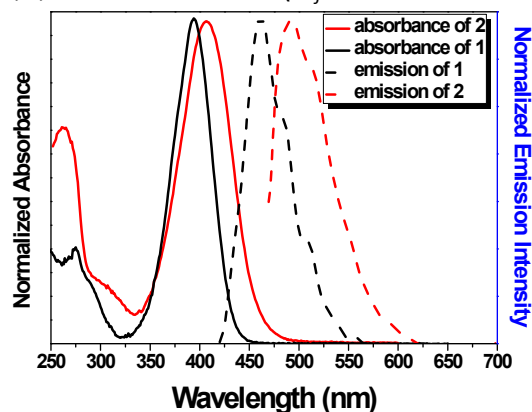


Figure S1. Normalized absorption and luminescence spectra of compounds **1** (10^{-5} M) and **2** (10^{-5} M) in CH_2Cl_2 .

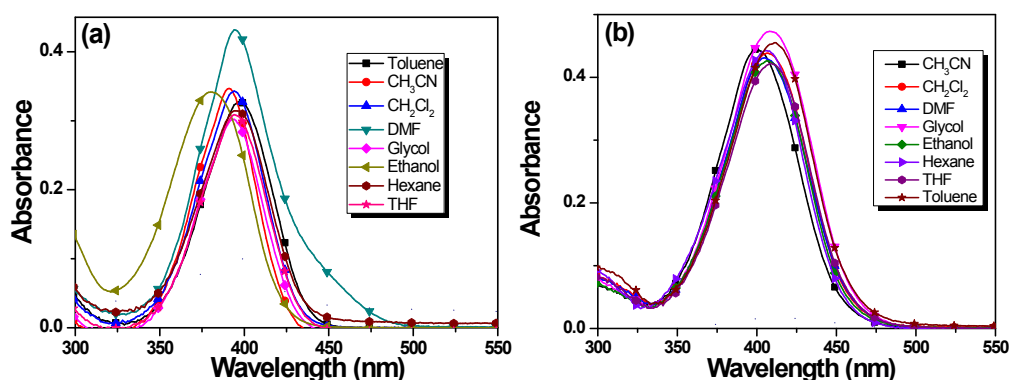


Figure S2. Absorption spectra of compounds **1** (a, 10^{-5} M) and **2** (b, 10^{-5} M) in different solvents.

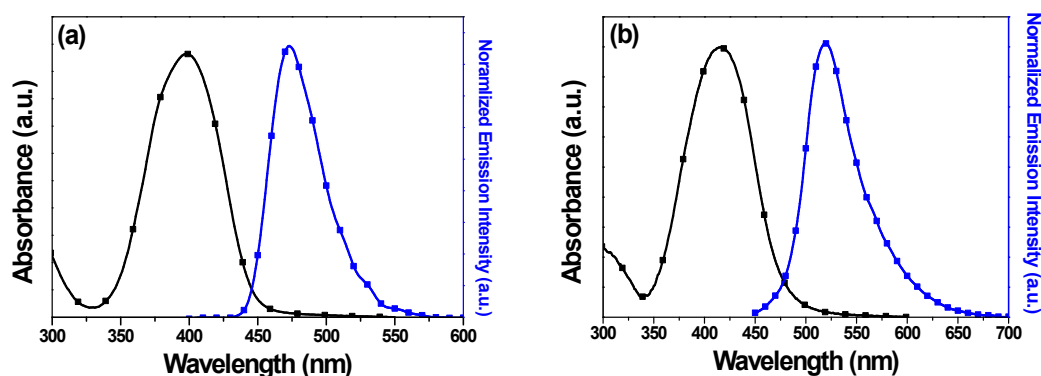


Figure S3. Normalized absorption and luminescence spectra of compounds **1** (a) and **2** (b) in solid state.

Table S1. Absorption/luminescence data of compounds **1** and **2** in solution or solid

state.

	In Solution ^a				In the solid state				
	λ_{abs} (nm) ^b	ε (M ⁻¹ cm ⁻¹) ¹	λ_{em} (nm) ^c	Φ_f (%) ^d	λ_{abs} (nm)	λ_{em} (nm)	Φ_f (%) ^e	λ_{em} (nm) ^f	$\Delta\lambda_{\text{em}}$ ^g
1	395	34200	458	0.46	406	473	0.60	481	8
2	409	43800	522	0.10	414	518	0.27	582	64

^a Measured at a concentration of 10 μM at 25 °C; ^b data in CH_2Cl_2 ; ^c data in glycerol; ^d Quantum yield in glycerol; ^e absolute quantum yield determined by calibrated integrating sphere systems; ^f emission band of ground powder; ^g red shift of luminescence induced by grinding.

4. Luminescent response of compounds 1 and 2 to the mechanical grinding

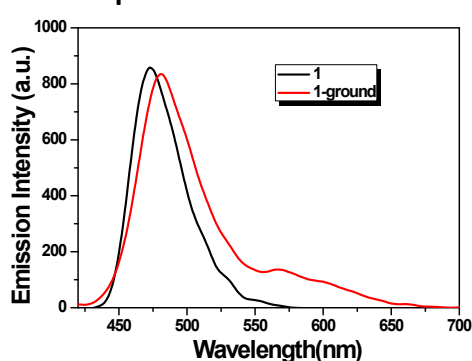


Figure S4. Luminescence spectra of compound **1** in solid state and after being ground.

Powder X-ray diffraction analysis of compounds 1 and 2 before and after grinding

Powder X-ray diffraction analysis of compounds **1** and **2** were carried out with a Bruker D8 Advance X-ray diffractometer with monochromated $\text{CuK}\alpha$ radiation. Ground powder was prepared by using an agate mortar with grinding time of 20 min.

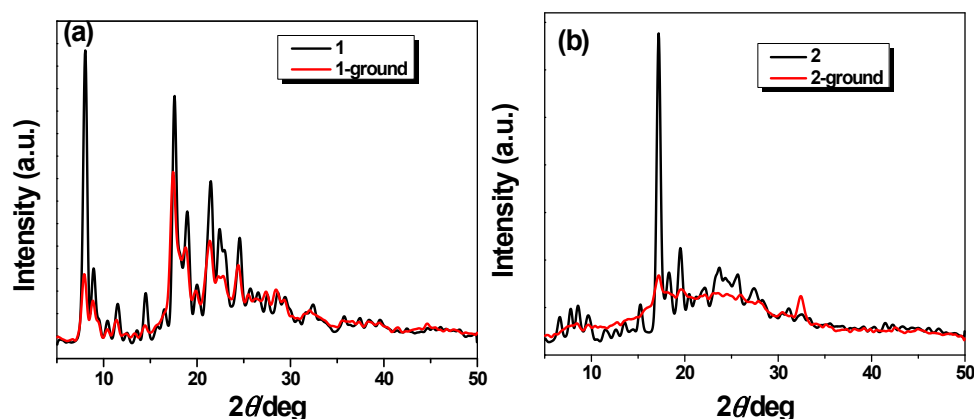


Figure S5. Powder XRD patterns of compounds **1** (a) and **2** (b) in solid state. The red lines are for the ground powders, and the black lines for powders before grinding.

5. Luminescence of compounds 1 and 2 upon hydrostatic compression

The hydrostatic compression to ~ 10 GPa was conducted at room temperature in a diamond anvil cell. Stainless steel gaskets, 50 μm in thickness with holes 120 μm in diameter, were used as the chambers for loading the samples. A 4:1 mixture of methanol and ethanol was used as a pressure transmission medium (PTM). The high

pressure photoluminescence measurements were carried out on a QuantaMaster 40 spectrometer in the reflection mode. The 405 nm line of a violet diode laser with a spot size of 20 μm and a power of 100 mW was used as the excitation source. A Nikon fluorescence microscope was used to focus the laser on the sample loaded in the diamond anvil cell. The emission spectra were recorded with a monochromator equipped with a photomultiplier (PMT).

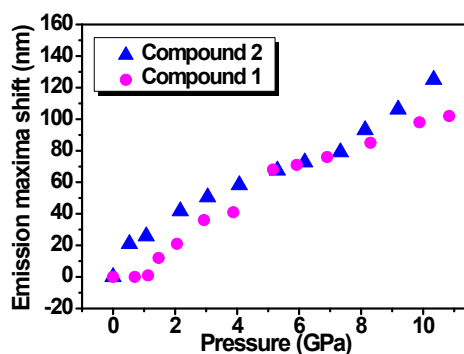


Figure S6. Pressure dependent luminescence shift of compounds **1** and **2** induced by hydrostatic compression.

6. X-ray crystallographic analysis

Crystal structure of compound 1

Green and prism single crystals of compound **1** were crystallized from a solution of CH_2Cl_2 . Intensity data were collected at 293 K on a Gemini A Single Crystal CCD X-ray diffractometer with $\text{MoK}\alpha$ radiation ($\lambda = 0.71073 \text{ \AA}$) and graphite monochromator. The structure was solved by direct methods (SHELX-97)^[2] and refined by the full-matrix least-squares on F_2 (SHELX-97). All the non-hydrogen atoms were refined anisotropically and all the hydrogen atoms were placed by using AFIX instructions. Crystal data: Formula $\text{C}_{27}\text{H}_{19}\text{BF}_2\text{N}_2\text{S}$, MW = 452.32, triclinic, $P-1$, $a = 10.1096(5)$, $b = 12.4472(13)$, $c = 18.3814(9) \text{ \AA}$, $\alpha = 95.587(6)^\circ$, $\beta = 95.919(4)^\circ$, $\gamma = 96.900(6)^\circ$, $V = 2269.9(3) \text{ \AA}^3$, $Z = 4$, $D_{\text{calc}} = 1.324 \text{ g.cm}^{-3}$; $\mu = 0.177 \text{ mm}^{-1}$; $R_1 (I > 2\sigma(I)) = 0.0670$, wR_2 (all data) = 0.1832, GOF = 1.012. Total 15241 reflections were collected, among which 7977 reflections (595 parameters) were independent ($R_{\text{int}} = 0.0408$). CCDC-1005620.

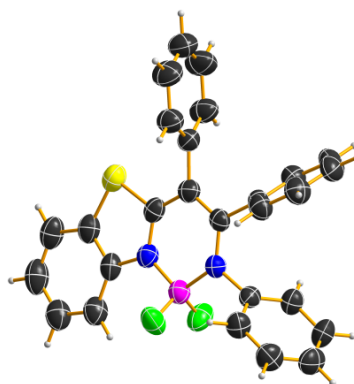


Figure S7. Molecular structure of compound **1** (50% probability for thermal ellipsoids).

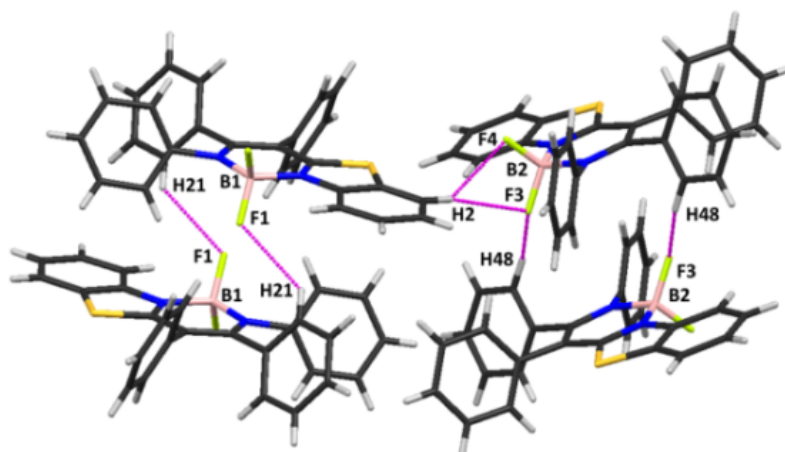


Figure S8. Molecule packing mode in the crystal structure of compound **1**. The pink lines showed the intermolecular hydrogen-bonds.

Crystal structure of compound 2

Yellow and prism single crystals of **2** were grown from a solution of THF. Intensity data were collected at 293 K on a Gemini A Single Crystal CCD X-ray diffractometer with $\text{MoK}\alpha$ radiation ($\lambda = 0.71073 \text{ \AA}$) and graphite monochromator. The structure was solved by direct methods (SHELX-97)^[2] and refined by the full-matrix least-squares on F_2 (SHELX-97). All the non-hydrogen atoms were refined anisotropically and all the hydrogen atoms were placed by using AFIX instructions. Crystal data: Formula $\text{C}_{66}\text{H}_{66}\text{B}_2\text{F}_4\text{N}_8\text{OS}_2$, $MW = 1149.01$, monoclinic, $C 2$, $a = 29.997(3)$, $b = 8.4716(9)$, $c = 12.7084(11) \text{ \AA}$, $\alpha = 90^\circ$, $\beta = 112.788(2)^\circ$, $\gamma = 90^\circ$, $V = 2977.4(5) \text{ \AA}^3$, $Z = 2$, $D_{\text{calc}} = 1.282 \text{ g.cm}^{-3}$, $\mu = 0.153 \text{ mm}^{-1}$; $R_1 (I > 2\sigma(I)) = 0.0587$, $wR_2 (\text{all data}) = 0.1548$, $\text{GOF} = 0.923$. Total 7583 reflections were collected, among which 5112 reflections (421 parameters) were independent ($R_{\text{int}} = 0.0502$). CCDC-1005623.

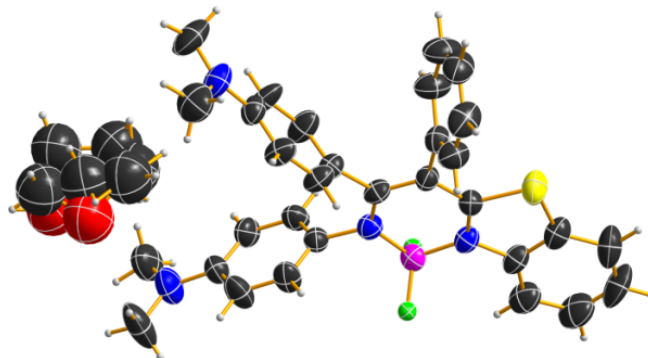


Figure S9. Molecular structure of compound **2** (50% probability for thermal ellipsoids).

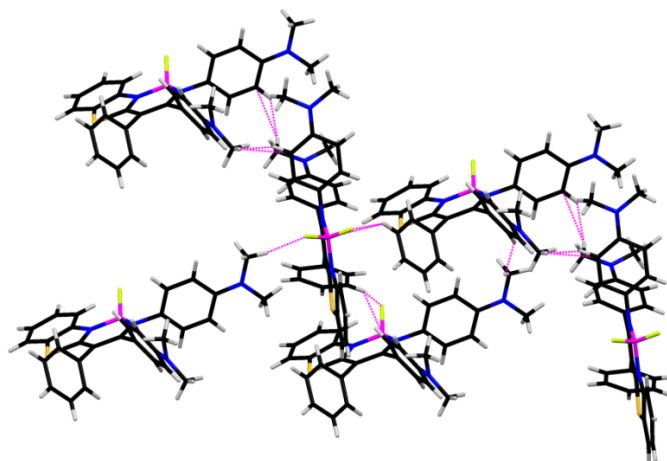


Figure S10. Molecule packing mode of compound **2**. The pink dotted lines show intermolecular hydrogen-bond and C-H... π interactions within compound **2**. THF molecule was omitted for clarify.

7. Single-point DFT calculations of Compounds **1** and **2**.

TD-DFT calculations were performed at the hybrid density functional theory level (B3LYP) with the 6-31G(d,p) basis set, using the Gaussian03 software package. The calculations were made in the gas phase.^[3]

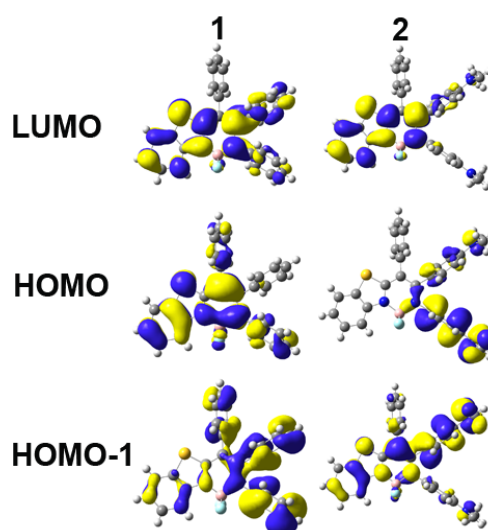


Figure S11. The virtual MOs for compounds **1** and **2** at the B3LYP/6-31G(d,p) level.

8. Molecular packing modes optimized by DFT

The packing geometries of compounds **1** and **2** at 1.5 and 4.0 GPa were optimized by DFT calculations by the CASTEP code.^[4] The GGA-PBE exchange–correlation functional^[5] was used with the norm-conserving pseudopotentials.^[6] The energy cut-off for the plane wave basis set was 780.0 eV. The SCF energy tolerance was set to 5×10^{-7} eV per atom. For the geometry optimization the total energy convergence tolerance was 3.0×10^{-6} eV per atom, with a maximum force tolerance of 0.007 eV/Å, a maximum displacement of 3.0×10^{-4} Å, and a maximum stress tolerance of 0.01 GPa.^[7]

The powder of compound **1** showed the same XRD pattern as the simulated XRD pattern based on the single crystal X-ray diffraction analysis (Figure S12). Thus, the

packing geometries of compound **1** were optimized based on the crystal structures of compound **1**. The packing geometries of compound **2** were optimized based on the crystal structures of compound **2**, and the THF molecules within the crystal were omitted for clarification.

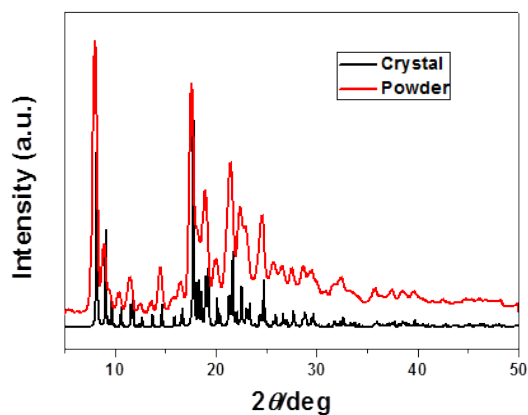


Figure S12. Powder XRD patterns of compound **1** in different solid-states.

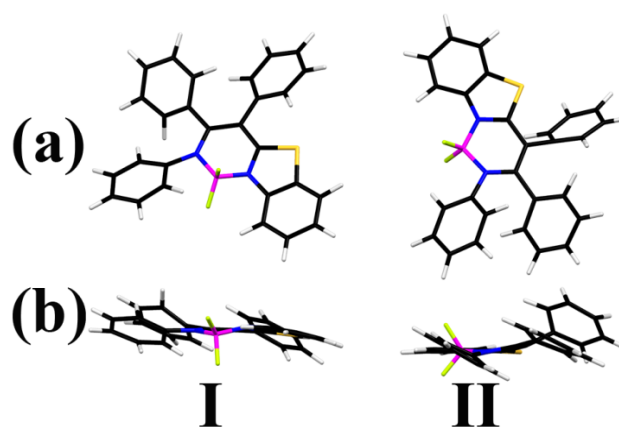


Figure S13. Top (a) and side (b) view of the optimized structures of compound **1** at 1.5 GPa.

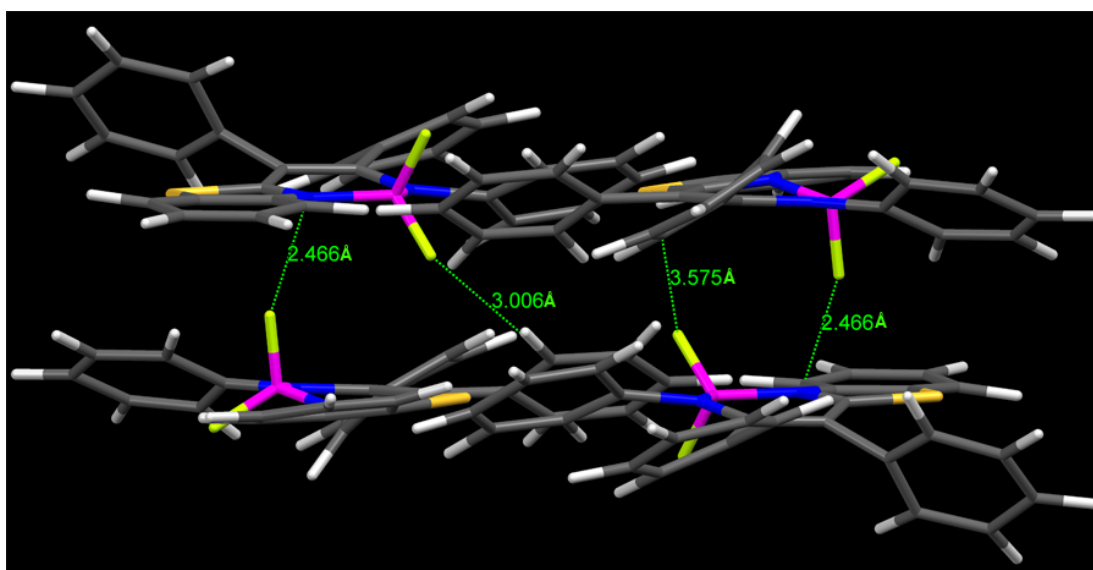


Figure S14. Optimized packing mode of compound **1** at 1.5 GPa. The green dotted lines show C-H...F interactions within compound **1**.

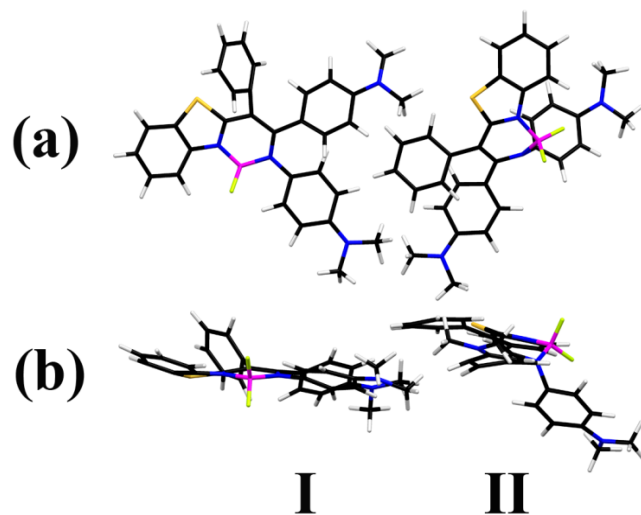


Figure S15. Top (a) and side (b) view of the optimized structures of compound **2** at 1.5 GPa.

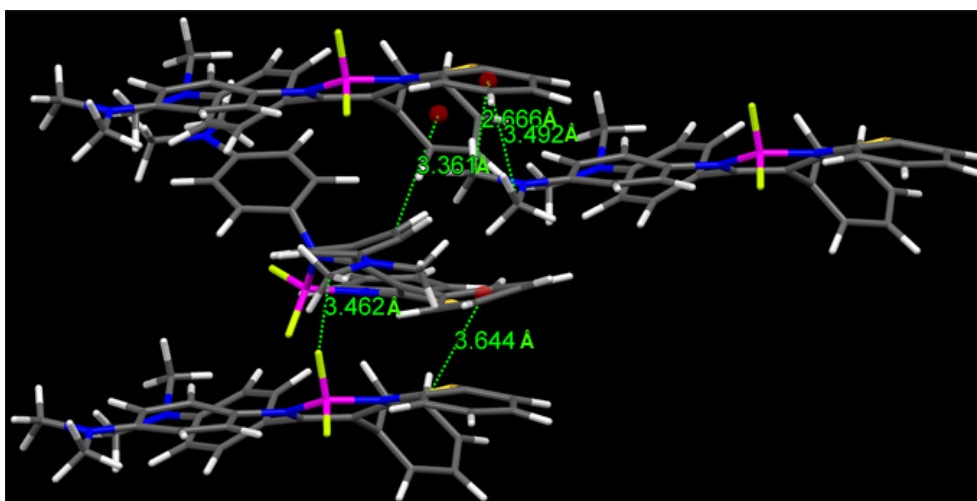


Figure S16. Optimized packing mode of compound **2** at 1.5 GPa. The green dotted lines show C–H...F and C–H... π interactions within compound **2**.

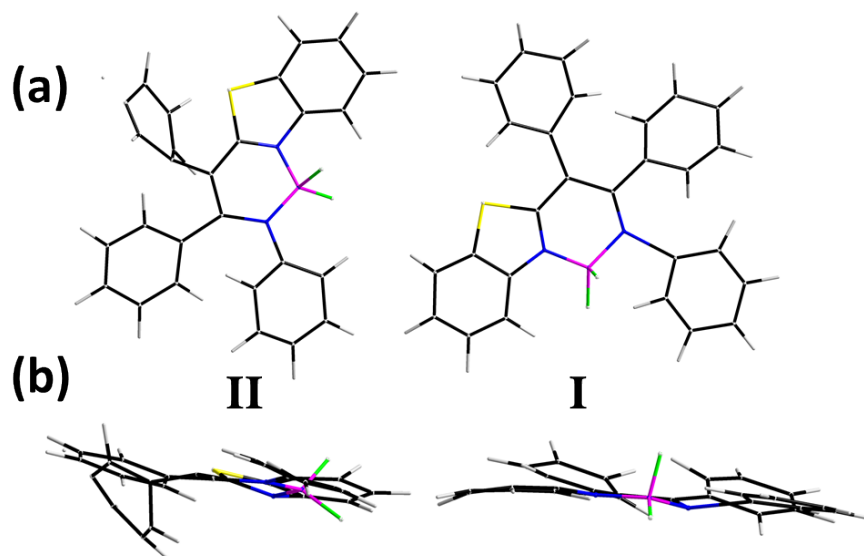


Figure S17. Top (a) and side (b) view of the optimized structures of compound **1** at 1.5 GPa.

4.0 GPa.

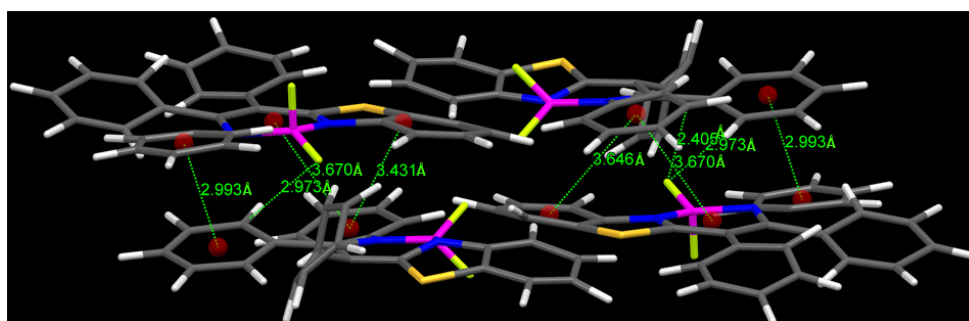


Figure S18. Optimized packing mode of compound **1** at 4.0 GPa. The green dotted lines show strong C–H... π and π – π interactions within compound **1**.

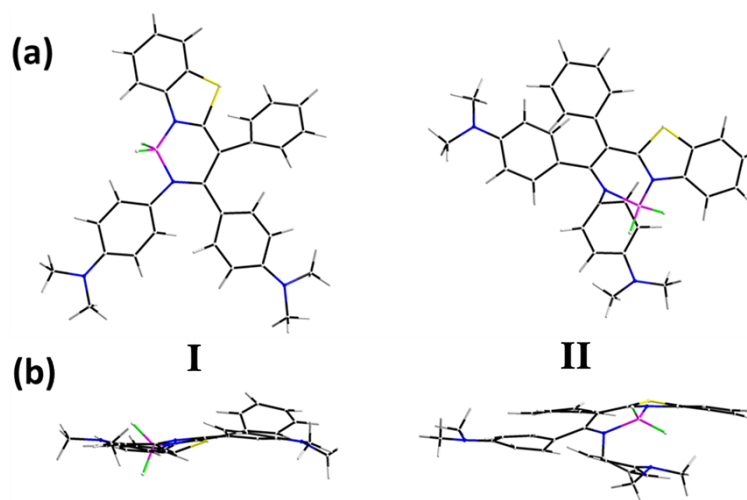


Figure S19. Top (a) and side (b) view of the optimized mode of compound **2** at 4.0 GPa.

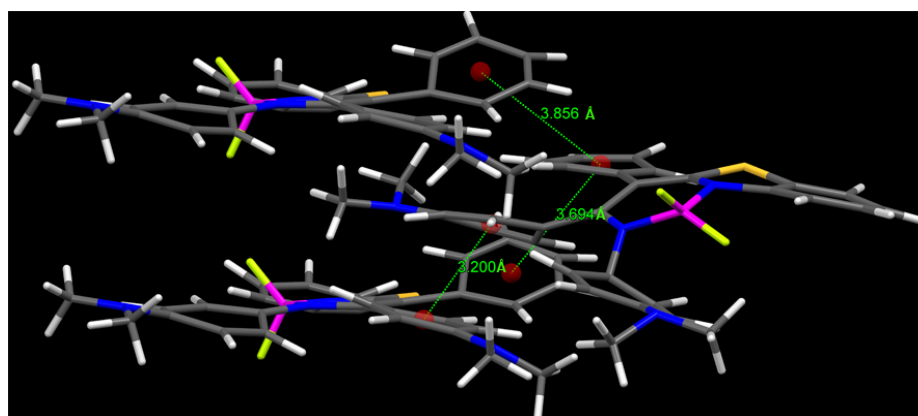


Figure S20. Optimized packing structure of compound **2** at 4.0 GPa. The green dotted lines show strong π – π interactions within compound **2**.

Table S2. Optimized lattice parameters of compound **1** at 1 atm, 1.5 and 4.0 GPa. ^a

Pressure	$a/\text{Å}$	$b/\text{Å}$	$c/\text{Å}$	$\alpha/^\circ$	$\beta/^\circ$	$\gamma/^\circ$
1 atm	10.1096	12.4472	18.3814	95.587	95.919	96.900
1.5 GPa	26.3352	21.2626	19.6165	101.7232	111.5284	142.9346
4.0 GPa	27.3207	23.2424	21.1948	116.1293	91.5646	151.4182

^a Calculated at the GGA-PBE level of theory.

Table S3. Optimized lattice parameters of compound **2** at 1 atm, 1.5 and 4.0 GPa. ^a

Pressure	<i>a</i> / Å	<i>b</i> / Å	<i>c</i> / Å	α / °	β / °	γ / °
1 atm	29.997	8.4716	12.708 4	90	112.788	90
1.5 GPa	50.271 5	11.2442	19.225 0	103.2088	133.8398	117.5345
4.0 GPa	52.964 6	11.7682	20.865 6	98.1553	134.3324	125.4239

^a Calculated at the GGA-PBE level of theory.**Table S4.** Dihedral angles of the **D** ring with **A**, **B**, and **C** rings in the optimized modes of compound **1**. ^a

Pressure	I			II		
	<i>A</i> / °	<i>B</i> / °	<i>C</i> / °	<i>A</i> / °	<i>B</i> / °	<i>C</i> / °
1 atm	72.03	65.60	61.00			
1.5 GPa	32.99	36.30	27.65	48.41	30.16	34.20
4.0 GPa	8.09	21.87	22.61	59.36	12.08	7.57

^a Calculated at the GGA-PBE level of theory.**Table S5.** Dihedral angles of the **D** ring with **A**, **B**, and **C** rings in the optimized mode of compound **2**. ^a

Pressure	I			II		
	<i>A</i> / °	<i>B</i> / °	<i>C</i> / °	<i>A</i> / °	<i>B</i> / °	<i>C</i> / °
1 atm	73.63	73.56	83.16			
1.5 GPa	65.56	40.61	26.05	33.61	33.22	55.80
4.0 GPa	33.56	9	14.52	16.66	18.62	44.19

^a Calculated at the GGA-PBE level of theory.

9. Reference

- [1] Uchiyama, S.; Matsumura, Y.; de Silva, A. P.; Iwai, K. *Anal. Chem.* **2003**, *75*, 5926.
- [2] Sheldrick, G. M. SHELX-97, *Program for the Refinement of Crystal Structures*; University of Göttingen, Göttingen, Germany, 1997.
- [3] Gaussian 03, Revision B. 05, M. J. Frisch, G. W. Trucks, H. B. Schlegel, G. E. Scuseria, M. A. Robb, J. R. Cheeseman, J. A. Montgomery, Jr., T. Vreven, K. N. Kudin, J. C. Burant, J. M. Millam, S. S. Iyengar, J. Tomasi, V. Barone, B. Mennucci, M. Cossi, G. Scalmani, N. Rega, G. A. Petersson, H. Nakatsuji, M. Hada, M. Ehara, K. Toyota, R. Fukuda, J. Hasegawa, M. Ishida, T. Nakajima, Y. Honda, O. Kitao, H. Nakai, M. Klene, X. Li, J. E. Knox, H. P. Hratchian, J. B. Cross, V. Bakken, C. Adamo, J. Jaramillo, R. Gomperts, R. E. Stratmann, O. Yazyev, A. J. Austin, R. Cammi, C. Pomelli, J. W. Ochterski, P. Y. Ayala, K. Morokuma, G. A. Voth, P. Salvador, J. J. Dannenberg, V. G. Zakrzewski, S. Dapprich, A. D. Daniels, M. C. Strain, O. Farkas, D. K. Malick, A. D. Rabuck, K. Raghavachari, J. B. Foresman, J. V. Ortiz, Q. Cui, A. G. Baboul, S. Clifford, J. Cioslowski, B. B. Stefanov, G. Liu, A. Liashenko, P. Piskorz, I. Komaromi, R. L. Martin, D. J. Fox, T. Keith, M. A. Al-Laham, C. Y. Peng, A. Nanayakkara, M. Challacombe, P. M. W. Gill, B. Johnson, W. Chen, M. W. Wong, C. Gonzalez, and J. A. Pople, Gaussian,

Inc., Pittsburgh, PA, **2003**.

[4] Clark, S. J.; Segall, M. D.; Pickard, C. J.; Hasnip, P. J.; Probert, M. I. J.; Refson, K.; Payne, M. C.; *Z. Kristallogr.* **2005**, *220*, 567.

[5] Perdew, J. P.; Burke, K.; Ernzerhof, M. *Phys. Rev. Lett.* **1996**, *77*, 3865.

[6] Vanderbilt, D. *Phys. Rev. B* **1990**, *41*, 7892.

[7] Tkatchenko A.; Scheffler, M. *Phys. Rev. Lett.* **2009**, *102*, 073005.

10. NMR spectra

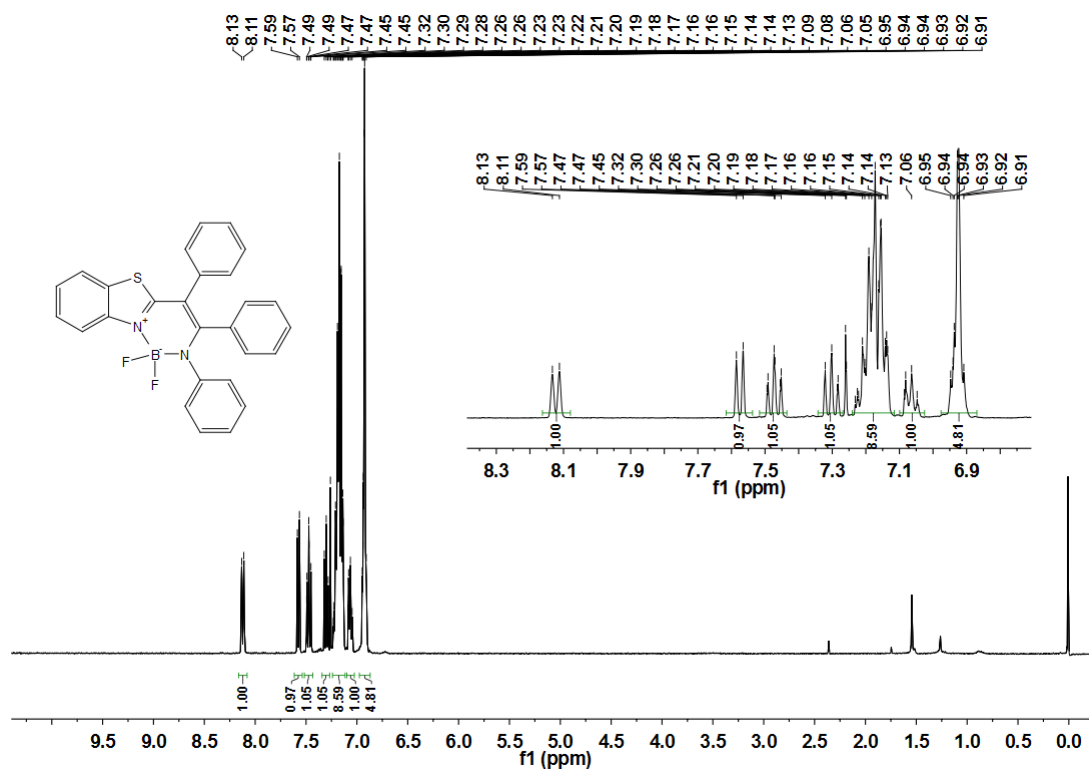


Figure S21. ¹H NMR of compound **1** in CDCl₃.

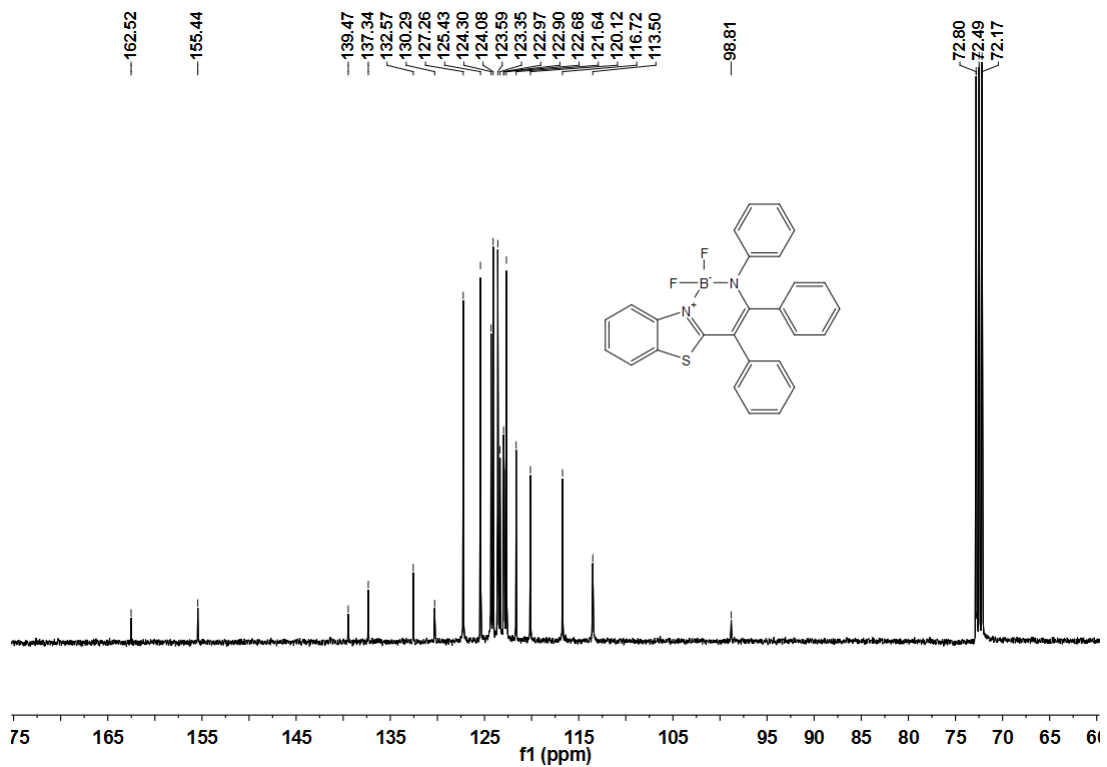


Figure S22. ¹³C NMR of compound 1 in CDCl₃.

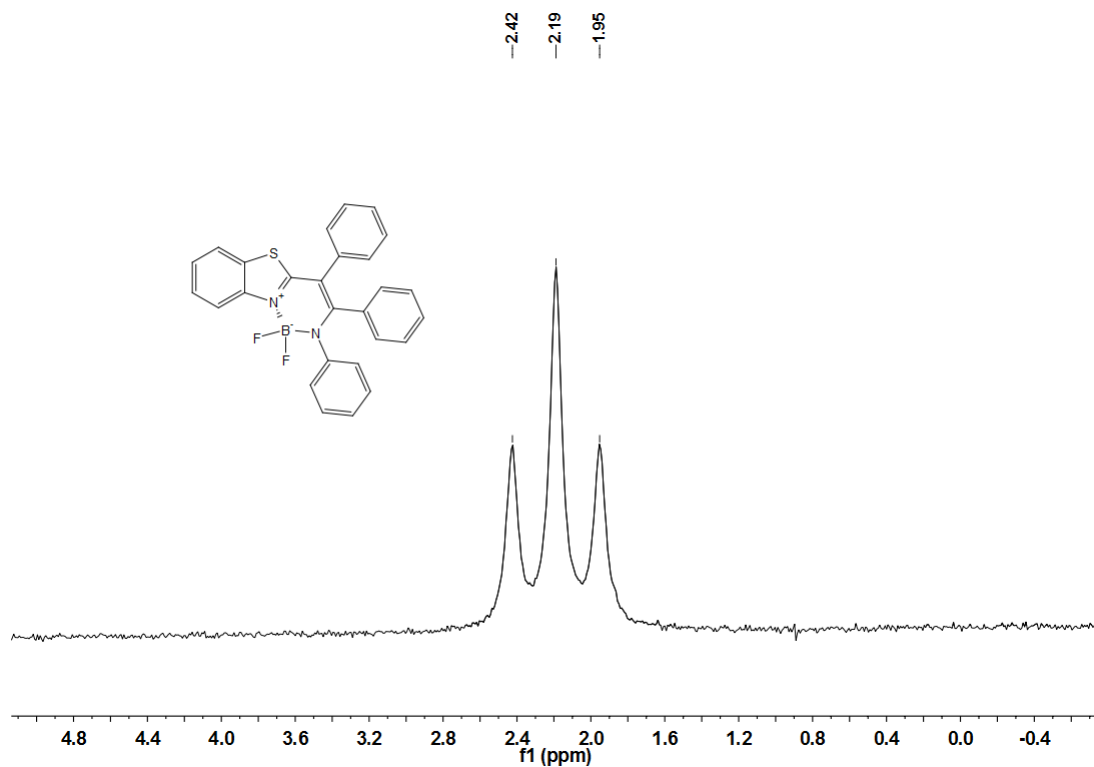


Figure S23. ¹¹B NMR of compound 1 in CDCl₃.

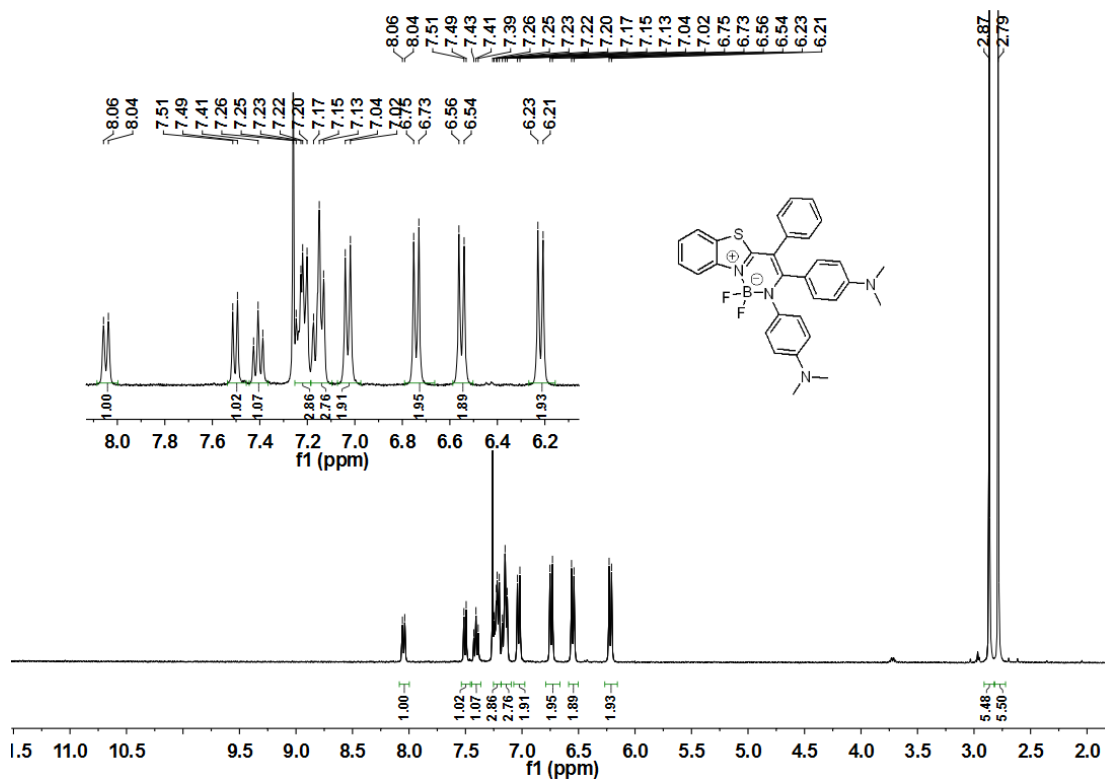


Figure S24. ^1H NMR of compound 2 in CDCl_3 .

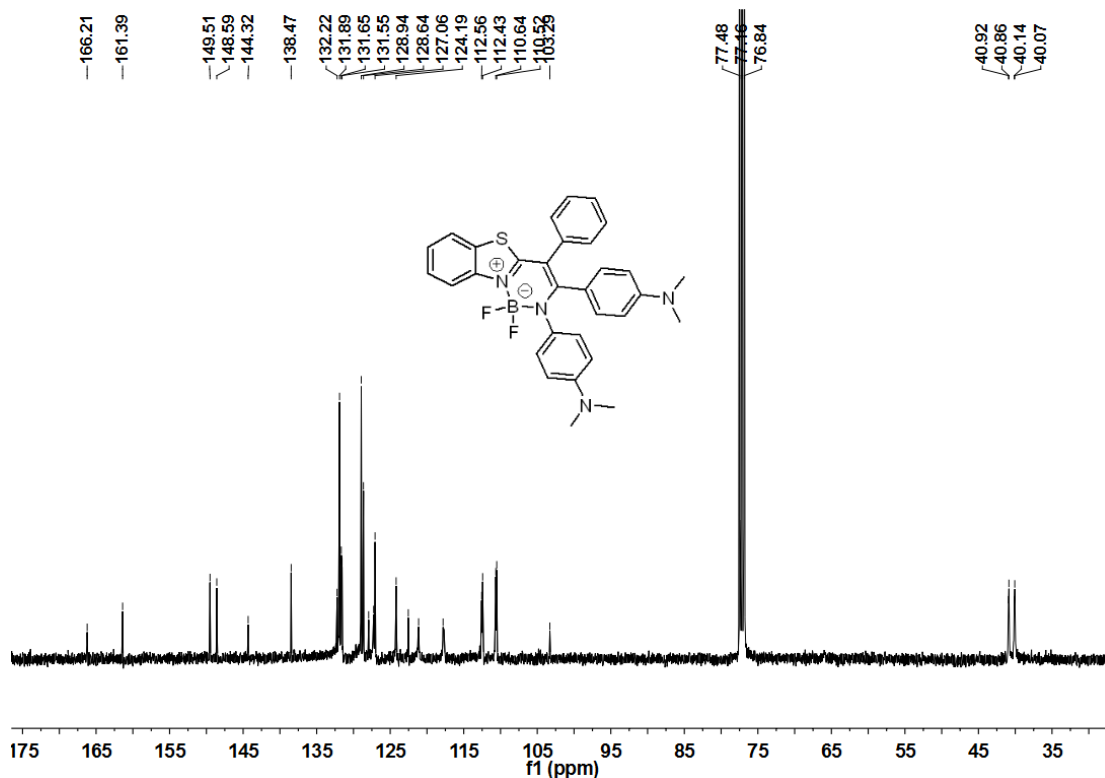


Figure S25. ^{13}C NMR of compound 2 in CDCl_3 .

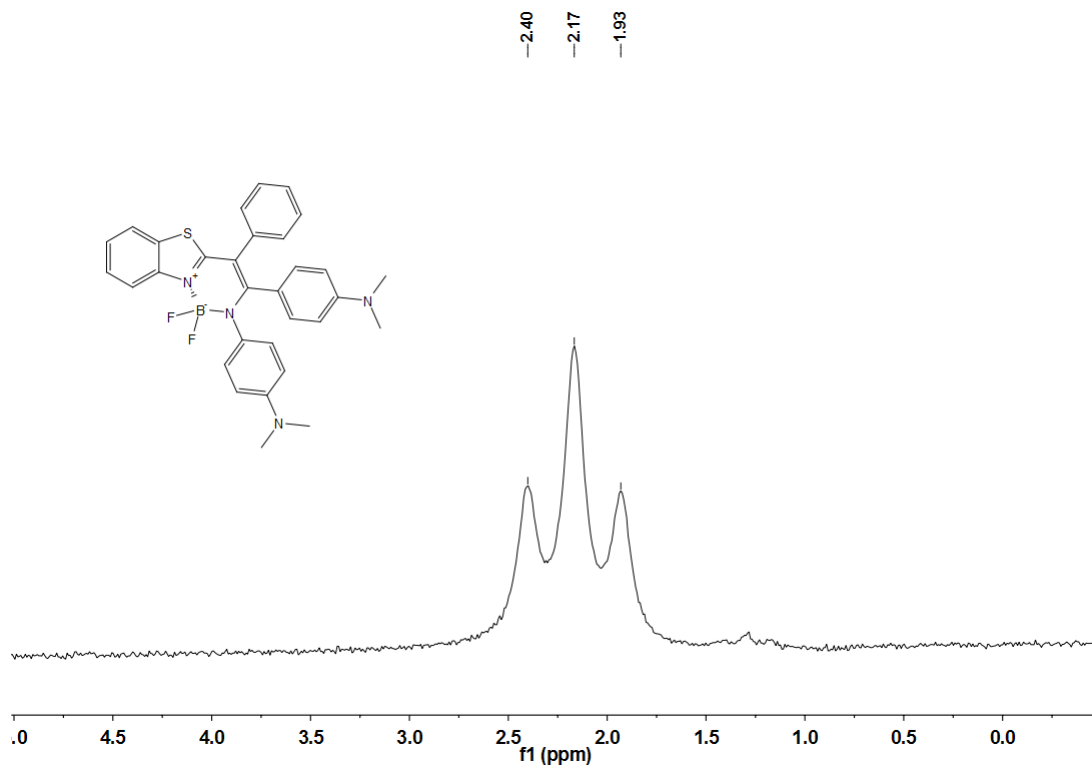


Figure S26. ^{11}B NMR of compound **2** in CDCl_3 .